Catalysis Today 418 (2023) 114054

Contents lists available at ScienceDirect

Catalysis Today

journal homepage: www.elsevier.com/locate/cattod

Insights on butyl levulinate bio-blendstock: From model sugars to paper mill waste cellulose as feedstocks for a sustainable catalytic butanolysis process

Anna Maria Raspolli Galletti [a,b], Rosaria Lorè [a], Domenico Licursi [a,b], Nicola Di Fidio [a,b], Claudia Antonetti [a,b], Sara Fulignati [a,b,*]

[a] Department of Chemistry and Industrial Chemistry, University of Pisa, Via G. Moruzzi 13, 56124 Pisa, Italy
[b] Consorzio Interuniversitario Reattività Chimica e Catalisi (CIRCC), Via Celso Ulpiani 27, 70126 Bari, Italy

ARTICLE INFO

Keywords:
Alcoholysis
Butyl levulinate
Bio-fuel
Cellulose powder
Char characterization

ABSTRACT

Butyl levulinate (BL) represents a novel diesel bio-blendstock and a versatile intermediate and solvent. The one-pot acid-catalyzed conversion of C6-feedstocks, employing *n*-butanol as the solvent/reagent, implies the upgrading of low-cost or, even better, waste biomasses for developing prompt process intensification. In this paper, the one-pot butanolysis process has been studied, moving from model glucose and microcrystalline cellulose to a waste cellulose feedstock deriving from a real papermaking process. The performances obtained with this waste biomass have been optimized, achieving BL yields up to 46 mol %, adopting a high-gravity approach, in the presence of diluted sulfuric acid as the catalyst. The optimization was carried out also in the perspective of minimizing the alcohol etherification to dibutyl ether, and the feedstock carbonization to char by-product, whose characterization was performed to identify its suitable applications. The combined production of both BL as a valuable bio-fuel and char as an exploitable carbonaceous bio-material can pave the way to the development of the one-pot butanolysis of real cellulosic or lignocellulosic biomasses in an environmentally sustainable and integrated perspective, in agreement with the principles of the circular bio-economy.

1. Introduction

Cellulosic and lignocellulosic biomasses represent renewable resources for the production of biofuels and chemicals, which otherwise should derive from dwindling fossil sources [1–3]. In this context, alkyl levulinates (ALs) are emerging as strategic bio-products, finding applications as oxygenated bio-fuels, fragrances, plasticizers, intermediates for chemical and pharmaceutical industry, food additives and bio-solvents [4–6]. These compounds can be advantageously upgraded into more valuable bio-products, such as ketals [7], alkoxypentanoates [8] and γ-valerolactone [9,10], due to the greater stability of the ester (respect to levulinic acid), which generally reduces the formation of by-products [11,12]. Regarding the ALs production, different strategies are available, the first one providing a two-step process that involves the preliminary acid-catalyzed hydrothermal conversion of cellulose to LA, which is subsequently purified and hence esterified with the alkyl alcohol, adopting a suitable esterification catalyst (path A, Fig. 1) [13]. The second possibility is a multi-step route involving the preliminary acid-catalyzed hydrolysis of the hemicellulose fraction (mainly xylans) to simpler C5 monosaccharides (i.e. xylose), which are in turn dehydrated to furfural, hydrogenated to furfuryl alcohol and converted to ALs by alcoholysis, always in the presence of a suitable acid catalyst (path B, Fig. 1) [13]. These pathways are shown in Fig. 1:

In addition to the above mentioned possibilities, if path A is carried out in an alcohol medium, rather than in water, it is possible to directly perform the conversion of C6 feedstocks to ALs by alcoholysis route (path C, Fig. 1), whose reaction mechanism is similar to that of the traditional hydrothermal process for LA production, but showing improved selectivity to the target product (ALs), mainly due to a reduced formation of furanic reaction by-products, as humins [14,15]. In this context, direct alcoholysis of cheap real lignocellulosic biomasses is certainly preferred over that of more costly model compounds, to develop potentially sustainable and economically feasible ALs industrial processes. On the other hand, the study of the reactivity of simpler model molecules can be greatly helpful to better understand the role of the main reaction parameters on this process [16]. Up to now, direct

* Corresponding author at: Department of Chemistry and Industrial Chemistry, University of Pisa, Via G. Moruzzi 13, 56124 Pisa, Italy.
E-mail address: sara.fulignati@dcci.unipi.it (S. Fulignati).

https://doi.org/10.1016/j.cattod.2023.114054
Received 15 December 2022; Received in revised form 9 February 2023; Accepted 20 February 2023
Available online 21 February 2023

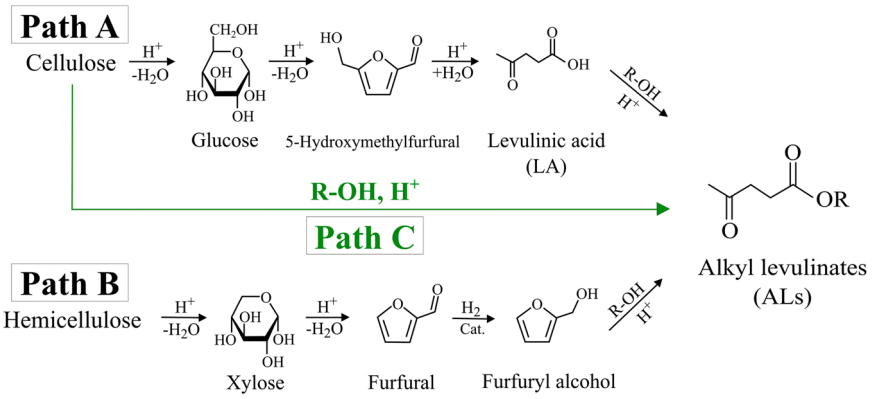

Fig. 1. Possible pathways for ALs production, starting from C6 and C5 carbohydrates/polysaccharides.

biomass alcoholysis has been applied especially to the depolymerization/liquefaction of the different biomass components, e.g. cellulose, hemicellulose and lignin, which can be converted into valuable reaction intermediates, such as alkyl glucosides/xylosides [17], furans [18] and aromatics [19], generally obtaining good yields. Remarkably, the direct biomass alcoholysis can be selectively addressed to Als [20] and, in this context, the research work has mainly aimed at the synthesis of short-chain ALs, in particular methyl levulinate (mL) [21] and ethyl levulinate (EL) [22,23]. Especially EL has been proposed as an efficient fuel additive, being advantageously used as a cold-flow improver in bio-diesel, as an oxygenated additive for gasoline and diesel fuels [24], and being its promising economic outlook recently demonstrated [22]. Actually, applied research is moving towards the synthesis of longer-chain ALs, to increase the hydrophobicity of these compounds, thus miming the structure of the fatty acid esters (bio-diesel) [25], to improve the energy density and water-insolubility [26,27]. However, the progressive increase of the carbon length makes both the esterification and the direct alcoholysis more difficult, due to steric hindrance issue [28]. Under this perspective, butyl levulinate (BL) represents an interesting compromise, thanks to its promising fuel properties, which are, in some cases, even better than those of EL [1,29,30] and to its feasible synthesis. In particular, the lower solubility in water, the good solubility in diesel fuel, and the impactful contribution to the reduction of the engine-out smoke number, make BL a more attractive diesel blend component than EL [1,31]. Regarding the catalysis issue, up to now, BL has been synthesized mainly by esterification of pure LA with butanol (BuOH) [32], but the direct butanolysis of model sugars or cellulosic biomasses is receiving increasing attention, because it does not require the intermediate LA purification, which is otherwise necessary when the successive esterification route is involved [33]. However, few studies reported, up to now, the direct butanolysis of glucose to BL adopting mainly *ad-hoc* synthesized heterogeneous catalysts and very low substrate loadings (1–6 wt %) [34–37]. Moreover, it is noteworthy that the few investigations up to now reported on glucose butanolysis have not studied the nature and amount of the involved by-products, but both represent key aspects for really optimizing the whole process.

In addition, the butanolysis of model cellulose has been reported only in a few works, adopting catalysts such as sulfuric acid [38–40], inorganic salts [34,41,42], solid acids [36], sulfated zirconia, or heteropolyacids as $Cs_2HPW_{12}O_{40}$ [43], and ionic liquids [44]. In each case, these catalysts showed low BL yields and/or other significant drawbacks (for example, ionic liquids have high costs of synthesis/recovery and unsolved environmental concerns), resulting unattractive for industrial application. Finally, the alcoholysis of real biomasses is still unexplored and only a very limited number of examples are available from the literature. In this context, Yamada et al. [45] proposed the alcoholysis of cellulosic biomasses, such as cellulose powder, kraft pulps, and papermaking sludges, to give butyl- pentyl- and hexyl-levulinates, adopting sulfuric acid as the catalyst. The absence of the lignin fraction makes the conversion of C6 carbohydrates present in these starting materials easier than that of lignocellulosic biomass and the authors claimed high yields to ALs, in the range of about 40–60 mol %, obtained by refluxing the different employed alcohols at their boiling points (117 °C, in the case of BL after 180 min), but a very high concentration of sulfuric acid (30 wt %), not sustainable from an environmental and applicative perspective, was necessary. In our previous work [46], the one-pot alcoholysis of *Eucalyptus nitens* biomass to BL has been carried out, achieving good BL molar yields (42 mol %), working in the presence of dilute sulfuric acid (1.9 wt %), at 183 °C for 146 min, under microwave (MW) heating. In the performed experiments, *n*-dibutyl ether (DBE) was always co-produced in significant amounts, even at a very low acid concentration (0.2 wt %). Despite the DBE formation is not generally mentioned in the literature, it must be considered because, if excessive, can represent a relevant drawback, indicating an undesired solvent loss. On the other hand, DBE can be also exploited as bio-fuel together BL, representing a very valuable ignition enhancer for low cetane bio-fuels, due to its high self-ignitability (cetane number = 100) [29]. In this context, our recent papers about the diesel engine performances/emissions for a ternary model mixture *n*-BuOH/BL/DBE have unequivocally confirmed its potential application as a valuable additive for diesel fuel, without any additional separation of the components [30,46].

In the present work, the BL synthesis has been further investigated, adopting a waste cellulosic biomass, namely a paper powder (PP) produced downstream of a papermill process, which cannot be re-used for the production of the tissue paper, thus resulting a waste. At the moment, the most common exploitation of cellulose-rich papermaking wastes is their combustion for the energy recovery, to use within the same papermill [47]. On the other hand, the choice of this waste biomass is certainly to be preferred for the BL production, due to its bulk prevalence of cellulose, absence of lignin, ready availability on the local territory and negative economic value. Due to this last aspect, cheap diluted sulfuric acid has been chosen as the catalyst, working at high substrate loading (high-gravity approach). In fact, all these conditions aim at the realisation of an economically sustainable process that allows the achievement of a good BL concentration in the reaction medium, although the maximisation of BL yield would require both the proper balance Brønsted and Lewis acidity, thus enhancing the isomerisation of glucose moieties to fructose and of the intermediate alkyl glucoside to alkyl fructoside [16], and the adoption of very low substrate concentration to reduce by-product formation. The optimization of the reaction conditions (temperature, time, and type of reactor) has been carried out on this waste cellulose and compared with the results obtained for model glucose and microcrystalline cellulose (MCC). Moreover, a preliminary characterization of the chars obtained from the cellulosic substrates has been performed, in order to propose their valorisation, in the perspective of developing a sustainable and integrated process.

2. Materials and methods

2.1. Materials

Waste paper powder (PP) was produced by Sofidel S.p.A. within the converting process for the production of tissue paper products and used after being dried in oven at 105 °C up to constant weight. Sulfuric acid (H_2SO_4, 95 wt %), *n*-butanol (*n*-BuOH, 94,5 %), *n*-dodecane (99 %), *n*-butyl levulinate (BL, 98 %), *n*-dibutyl ether (DBE, 99 %), microcrystalline cellulose powder (MCC, 99 %) and D-glucose (99.5 %) were purchased from Sigma-Aldrich and used as-received.

2.2. Chemical composition analysis of paper powder (PP)

The chemical composition of the paper powder was evaluated through the standard NREL protocols [48–51]. The procedure involves a preliminary hydrolysis of the biomass sample with 72 wt % sulfuric acid, performed at 30 °C for 1 h, followed by a hydrolysis of the obtained slurry with 4 wt % sulfuric acid, carried out at 121 °C for 1 h. The slurry was filtered through a ceramic crucible, and the filtered liquid phase was analyzed by HPLC, to determine the composition of the structural C5 and C6 carbohydrates. Regarding the insoluble residue recovered after the second hydrolysis step, it was dried up to constant weight, enabling the gravimetric quantification of the Klason (acid-insoluble) lignin. The ash content was determined as the percentage of residue recovered after dry oxidation of the starting biomass at 550 °C for 24 h. The determination of the extractive content was performed on 5 g of oven-dried PP samples, which were extracted in a Soxhlet apparatus for 24 h, with 200 mL of absolute ethanol.

2.3. X-ray diffraction analysis (XRD)

XRD analysis was carried out by a D8 Advance Bruker instrument. The analyses were performed using the CuK radiation. The interval of measurement was set in the range $5° < \theta < 80°$, with steps of 0.2°. The count of intensity was carried out every 2 s. Crystallinity index (CrI) of the starting feedstocks was evaluated after deconvolution of the acquired curves according to Park et al. [52] and calculated according to Eq. (1):

$$CrI=[1-(A_{AM}/A_{TOT})] \times 100 \quad (1)$$

where A_{AM} is the area of the peak corresponding to the amorphous cellulose and A_{TOT} is the total area of all peaks.

2.4. Scanning electron microscopy associated with energy-dispersion spectrometry (SEM/EDS)

SEM/EDS analysis was performed with a JEOL-6010/LA microscope. The EDS spectra were obtained using a working distance of 10 mm and a voltage of 20 KV.

2.5. Butanolysis experiments

Butanolysis experiments were carried out under traditional heating, adopting a Carius pressure tube or an autoclave reactor. In the first case, the reagents were added into a 60 mL Carius pressure tube (10.5 mL of *n*-butanol and the selected amount of substrate and catalyst), which was sealed, placed in a thermostated oil-bath, and the reaction slurry was maintained under magnetic constant stirring during the entire reaction. In the second case, an electrically heated 600 mL Parr zirconium-made fixed-head autoclave, which was equipped with a P.I.D. controller (4848), was used. The autoclave was pressurized with nitrogen up to 30 bar and the reaction mixture (100 mL of *n*-butanol and the selected amount of substrate and catalyst) was maintained under constant stirring during the entire reaction. In each run, *n*-dodecane was chosen as the internal standard and added into the reaction mixture before the reaction. At the end of each reaction, the reactors were cooled at room temperature by blown air, then the solid-liquid slurry was filtered under vacuum and the recovered liquid was properly diluted by acetone before the analysis, whereas the solid residue was washed by water and then dried at 105 °C for 24 h.

Substrate and catalyst loadings have been defined according to Eqs. (2) and (3):

$$\text{Substrate loading (wt \%)} = [g_{substrate}/(g_{substrate} + g_{catalyst} + g_{BuOH})] \times 100 \quad (2)$$

$$\text{Catalyst loading (wt \%)} = [g_{catalyst}/(g_{substrate} + g_{catalyst} + g_{BuOH})] \times 100 \quad (3)$$

2.6. Quantitative analysis of the reaction products

Quantitative analysis was carried out by Gas-Chromatography coupled with a Flame Ionization Detector (GC-FID), adopting the instrumentation and following the procedure described in our previous work [46]. Each analysis was carried out in triplicate, and the reproducibility was within 5 %. Molar and mass yields of BL and DBE were calculated according to Eqs. (4), (5), (6) and (7), respectively.

$$\text{Molar yield BL (mol \%)}=[(mol_{BL}/mol_{glucose\ or\ anhydroglucose\ unit\ in\ biomass})] \times 100 \quad (4)$$

$$\text{Mass yield BL (wt \%)}=[(g_{BL}/g_{starting\ feedstock})] \times 100 \quad (5)$$

$$\text{Molar yield DBE (mol \%)}=[(mol_{DBE}/mol_{n\text{-butanol}})] \times 100 \quad (6)$$

$$\text{Mass yield DBE (wt \%)}=[(g_{DBE}/g_{n\text{-butanol}})] \times 100 \quad (7)$$

Moreover, the mass yield of the solid residue recovered at the end of the reaction was calculated according to Eq. (8):

$$\text{Solid residue yield (wt \%)} = [(g_{solid\ residue}/g_{substrate})] \times 100 \quad (8)$$

2.7. Optical microscopy

Optical microscopy monitoring of raw biomass and hydrolysis residues was performed by a Stereo Discovery V8 Carl Zeiss™ microscope, with a manual 8x zoom.

2.8. Elemental analysis and HHV

Elemental analysis (C, H, N and O) of investigated samples was performed with an automatic analyzer C,H,N LECO TRUSPEC. Carbon and hydrogen contents were determined by infrared spectroscopy and nitrogen by thermal conductibility. Lastly, the oxygen content was calculated by difference: O (%) = 100 % − C(%) – H(%) – N(%). The reproducibility of this analysis was within 2 %. Lastly, the higher heating value (HHV) was calculated according to the correlation formula proposed by Channiwala and Parikh [53] and reported in Eq. (9):

$$\text{HHV (MJ/Kg)}=0.3491C(\%) + 1.1783H(\%) + 0.1005S(\%) - 0.1034O(\%) - 0.0151N(\%) - 0.0211\ Ash(\%) \quad (9)$$

2.9. FT-IR analysis

Fourier Transform-Infrared (FT–IR) characterization of the samples was carried out with a Perkin-Elmer Spectrum-Two spectrophotometer, equipped with an Attenuated Total Reflectance (ATR) accessory, working in the wavenumber range between 4000 and 450 cm^{-1}.

Table 1
Results of the glucose butanolysis performed in the Carius pressure tube.

Run	Glucose loading (wt %)	T (°C)	H_2SO_4 loading (wt %)	Time (h)	BL Molar yield (mol %)	BL Mass yield (wt %)	DBE Molar yield (mol %)	DBE Mass yield (wt %)	Solid residue yield (wt %)
G1	14	170	0.6	1	26	25	3	6	1
G2	14	170	0.6	3	39	38	6	11	6
G3	14	170	0.6	5	46	43	9	17	10
G4	14	170	0.6	8	41	39	13	23	18
G5	14	170	1.2	1	36	34	6	10	3
G6	14	180	0.6	1	34	33	6	10	5
G7	14	180	1.2	1	37	35	6	11	7
G8	22	170	0.6	1	23	22	3	5	0.4
G9	22	170	1.2	1	32	31	5	8	7

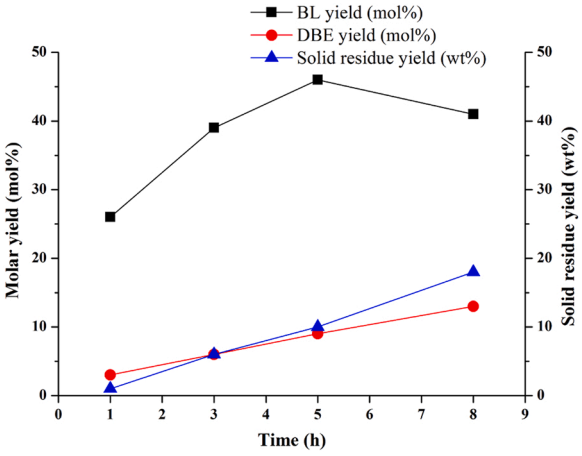

Fig. 2. Kinetics of glucose butanolysis reaction performed in the Carius pressure tube. Reaction conditions: 170 °C, glucose loading of 14 wt %, H_2SO_4 loading 0.6 wt %.

2.10. Specific surface area analysis

A single point ThermoQuest Surface Area Analyzer Qsurf S1 was used for the determination of the specific surface area of the chars. Before the measurement, the sample was treated at 130 °C for 12 h under a nitrogen flow. Subsequently, the sample was cooled down to the room temperature and then immersed into the liquid nitrogen for the measurement.

3. Results and discussion

3.1. Butanolysis of glucose

The preliminary study on glucose, herein considered as the model substrate, was performed in order to clarify important aspects of the one-pot butanolysis reaction which, up to now, are absolutely disregarded in the literature, but fundamental in the perspective of employing a waste biomass as PP. These aspects are the extent of ether and solid by-products formation and the possibility of employing high substrate loadings (14 and 22 wt %) in the presence of cheap diluted sulfuric acid (0.6 and 1.2 wt %) as the catalyst. The choice of this range of acid concentration has been made starting from corrosion and kinetics considerations, made on the basis of the practical experience and recent available literature on such acid-catalyzed processes, which is mostly focused on the diluted-acid approach [16,46], where corrosion is surely mitigated but not avoided. The obtained results are reported in Table 1.

The first run G1 was performed adopting a very low acid concentration (0.6 wt %) at 170 °C, with a glucose loading of 14 wt %, a much higher value respect to those up to now reported in the literature [34–37]. After 1 h of reaction, the BL yield of 26 mol % was ascertained, together with the parallel etherification of *n*-BuOH to DBE, the latter showing the yield of 3 mol %. The formation of a very low amount of solid by-product was also observed. The reaction time was then prolonged up to 8 h, to investigate the effect of this parameter on the BL

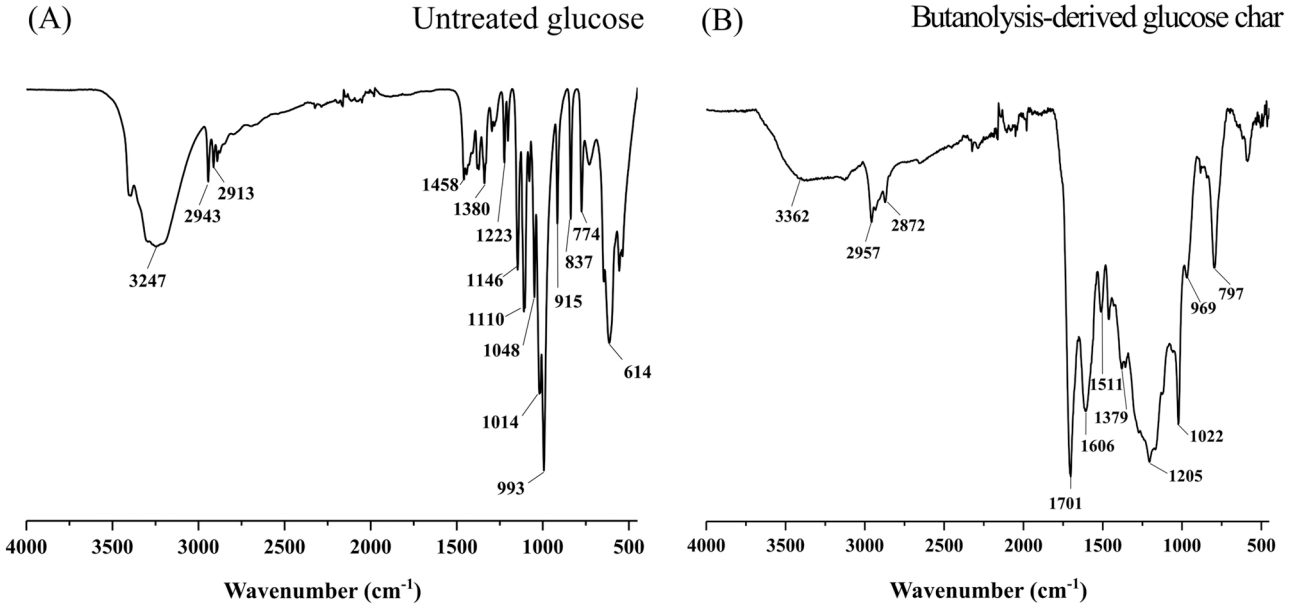

Fig. 3. FT-IR spectra of the starting glucose (A) and the corresponding butanolysis-derived char obtained from run G3 (B).

Table 2
Literature review on BL production starting from glucose.

Entry	Catalyst	Catalyst loading (wt %)	Glucose loading (wt %)	T (°C)	Time (h)	BL Molar yield (mol %)	Ref.
1	$Fe_2(SO_4)_3$	0.6	3	190	3	40	[34]
2	Zeolite H-USY (6)	1.8	3	160	20	12	[56]
3	SO_4^{2-}/SnO_2-ZrO_2+H_2SO_4	2.5+0.1	6	200	2	40	[36]
4	Zr/Al(2)-SB[a]	1.2	1	170	5	63	[37]
5	SO_4^{2-}/SnO_2	2.5	3	200	2	33	[57]
6	CMK-SOM[b]	1.0	2	200	5	65	[58]
7	H_2SO_4	0.6	14	170	5	46	This work

[a] Bimetallic Zr/Al catalyst supported on SBA-15 mesoporous silica.
[b] Ordered mesoporous carbon CMK-3 sulfonated with mercaptopropyltriethoxy silane.

yield (runs G1–G4, Table 1 and Fig. 2).

In the first 5 h, a progressive increase of the BL yield up to 46 mol % was observed, which represents a relevant achievement, considering the adopted cheap commercial catalyst and the high substrate loading, the latter generally avoided, due to the larger formation of condensation by-products. A further increase of the reaction time up to 8 h, caused a decrease of BL yield and, above all, the amount of DBE and of the recovered solid by-products reached significant values, accounting for 23 wt % of the starting *n*-BuOH and for 18 wt % of the starting glucose, respectively. When the amount of the acid catalyst was doubled (run G5, Table 1), the increase of the BL yield was counterbalanced by the significant increase of formed DBE and solid by-products, in addition to corrosion and catalyst recovery problems. On the other hand, the increase of the temperature to 180 °C had a positive effect on BL yield, in particular when the lower amount of acid was adopted (compare run G6 with run G1, Table 1), while the temperature scarcely influenced the catalytic performances in the presence of sulfuric acid concentration of 1.2 wt % (run G7, Table 1), where the yield to BL remained analogous to that ascertained in the run at 170 °C (compare run G7 with run G5, Table 1), but the extent of solid formation was significantly increased (from 3 wt % in run G5 to 7 wt % in run G7). The glucose loading was further increased from 14 to 22 wt % and, as expected, the BL molar yield slightly decreased for both the adopted acid concentrations (compare runs G8 and G9 with runs G1 and G5, respectively), this downside being offset by the enhancement of the concentration of BL in the reaction medium of more than 60 %. This result does not appear cost-effective when model glucose is employed as starting material, but it becomes profitable when the alcoholysis of a waste biomass as PP is performed.

The recovered solid by-products were characterized through FT-IR to identify their chemical structure. All the obtained spectra showed the same characteristic adsorption bands, thus the spectrum of the solid recovered from run G3 is reported as an example in Fig. 3, together with that of the starting glucose.

The FT-IR spectrum of glucose includes the absorption bands of O–H stretching at about 3362 cm^{-1}, together with symmetrical and asymmetrical stretching of methyl and methylene groups at 2957 and 2872 cm^{-1}, respectively, which are also present in the spectrum of the butanolysis-derived glucose char [54]. Moreover, the band at 1146 cm^{-1} is assigned to the C–O–C stretching and those between 1110 and 837 cm^{-1} to the ring vibrations of glucose. All these bands are not visible in the IR spectrum of the char, thus proving its different chemical structure. In fact, the absorption bands typical of aromatic/furanic systems are the most relevant bands in the char spectrum. In particular, absorption bands at 1606 cm^{-1} (aromatic skeletal vibration and C═O stretching), 1511 cm^{-1} (C═C stretching of aromatic/furanic compounds), 1379 cm^{-1} (C–O–C stretching of furan rings), and 797 cm^{-1} (C–H out-of-plane bending of furans) are present in the spectrum of the butanolysis-derived glucose char [54,55]. These evidences prove the formation of a furanic/aromatic solid residue, such as humins, as a consequence of the butanolysis process. Moreover, the existence of oxygenated functionalities is also confirmed by the presence of the absorption band at 1701 cm^{-1}, assigned to the stretching of C═O of carbonyls, and at 1205 and 1022 cm^{-1}, assigned to and the stretching of C–O of ethers [54].

The best result, in terms of BL molar yield, obtained in the present work (entry 7, Table 2) was compared with those already reported in the literature for the butanolysis of glucose to BL (Table 2).

All the previous studies reported in the literature were performed in the presence of a very low glucose concentrations (1–6 wt %), adopting homogeneous or *ad-hoc* synthesized heterogeneous acid catalysts, achieving BL yields in the range of 12–65 mol %. The two references, which report higher yields respect to the present research (entries 4 and 6, Table 2), involve the adoption not only of much lower substrate loadings, but also of *ad-hoc* synthesized heterogeneous catalysts, which are not suitable for the conversion of a solid waste substrate as PP, which will be investigated below. The use of low concentrations of glucose favors its conversion and the BL yield but produces diluted streams of BL that require high energy cost for the product separation, thus limiting the economic sustainability and the feasibility of the scale-up at

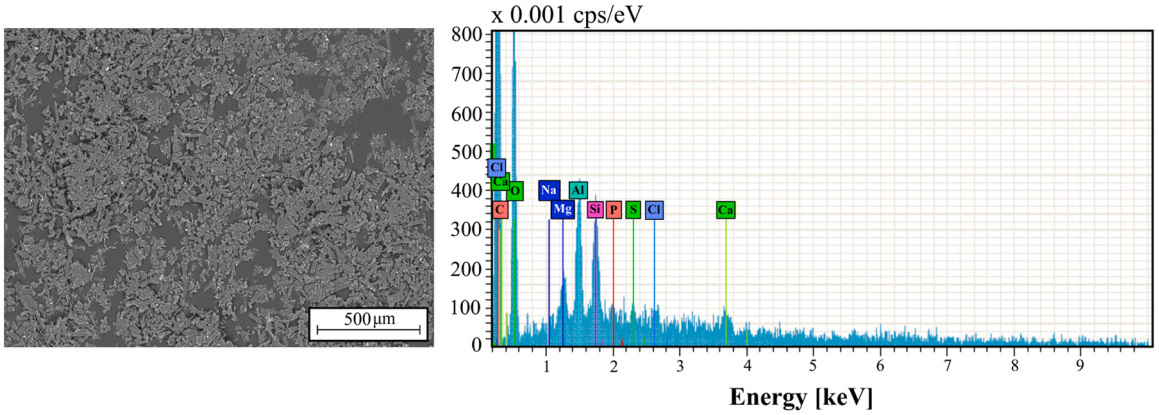

Fig. 4. SEM/EDS analysis of the raw PP.

Table 3
Results of the PP butanolysis: comparison between Carius and the autoclave. Reaction conditions: PP loading of 14 wt %.

Run	T (°C)	Type of reactor	H_2SO_4 loading (wt %)	Time (h)	BL Molar yield (mol %)	BL Mass yield (wt %)	DBE Molar yield (mol %)	DBE Mass yield (wt %)	Solid residue yield (wt %)
PP1	190	Carius	1.2	1	35	28	7	12	28
PP2	190			3	42	34	13	23	31
PP3	190		0.6	1	14	11	3	6	22
PP4	190			3	29	24	7	12	23
PP5	190			5	33	26	10	18	30
PP6	190			8	34	27	12	21	28
PP7	190	Autoclave	1.2	1	34	27	6	11	32
PP8	190			3	35	28	8	15	30
PP9	190			5	39	31	12	21	31
PP10	190		0.6	1	15	12	2	5	23
PP11	190			3	20	16	3	6	19
PP12	190			5	31	25	6	11	21
PP13	180			5	29	24	6	11	20
PP14	200			3	34	27	7	12	28

industrial level. To overcome this limit, in the present study the high-gravity approach was adopted in the butanolysis reaction, by using concentrations of glucose higher than 14 wt %. Despite the employment of substrate loading much higher than those adopted in the literature (entries 1–6, Table 2), the maximum BL yield obtained in this investigation reaches 46 mol % (entry 7, Table 2). Moreover, it is important to underline that this yield has been obtained in the presence of a very diluted commercial catalyst (0.6 wt % H_2SO_4) that makes easy a possible scale-up without overwhelming corrosion problems.

3.2. Butanolysis of the real and model cellulose feedstocks

The adopted PP feedstock derives from the converting cutting operations of a papermill process for the production of tissue paper. This fraction is currently considered as a waste material, because it cannot be reused within the same process. Its chemical composition was experimentally determined, resulting as follows: glucan (75.0 wt %), xylan (12.1 wt %), ashes (6.8 wt %), extractives (2.2 wt %) and lignin (3.9 wt %). High cellulose and low lignin contents make such biomass a promising feedstock for investigating the butanolysis reaction. On the other hand, the compositional analysis of the model microcrystalline cellulose (MCC) was also performed, confirming, as expected, the absence of bulk impurities. The determination of the CrI of the two raw feedstocks was carried out by the XRD technique (Fig. S1), amounting to 57 % and 62 % for PP and MCC, respectively. The lower CrI of PP is indicative of a lower recalcitrance towards conversion, thus further confirming the suitability of this cellulosic feedstock for BL production. Moreover, in the XRD spectrum of PP it is possible to identify the presence of $CaSO_4$, thus evidencing a higher amount of inorganic species in the PP rather than MCC. However, the SEM/EDS analysis of raw PP (Fig. 4 and Table S1) confirmed the low amount of elements different from carbon and oxygen, in particular aluminium (2.3 wt %) and silicon (1.7 wt %), responsible for the ascertained ashes.

When a waste biomass, as PP, is proposed for such a conversion strategy, high biomass loading should be proposed, thus increasing the BL concentration in the final liquor, aimed at simplifying the successive work-up operations and, definitely, at improving the process economy, in agreement with the high-gravity approach [59]. A loading of 14 wt %, analogous to that previously proposed for glucose, resulted optimal in a preliminary investigation (data not reported), whilst further increase of the biomass loading turned out to be practically infeasible, due to the fibrous and low-density texture of this feedstock, leading to mass transfer limitations, inefficient stirring and difficult recovery of the liquid phase after the reaction. The effect of the main reaction parameters on the PP butanolysis was studied, and the H_2SO_4 concentration appeared a key reaction variable for improving the process sustainability of the real biomass alcoholysis, where the adoption of low acid concentration at high temperature had be ascertained to be a proper

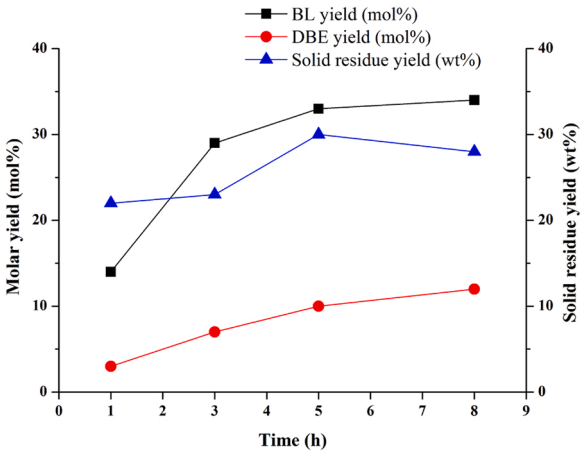

Fig. 5. Kinetics of PP butanolysis reaction in Carius pressure tube. Reaction conditions: 190 °C, PP loading of 14 wt %, H_2SO_4 loading 0.6 wt %.

choice [46]. The PP butanolysis was studied both in a Carius pressure tube and in an autoclave. The first one is generally preferred at laboratory-scale, due to its simple configuration but, from an industrial perspective, the use of the autoclave should be encouraged, representing a preliminary step towards scale-up, allowing to process larger amounts of substrate and to consider other reaction parameters, such as heat and mass transfer. As above reported for glucose, two catalyst loadings (1.2 and 0.6 wt %) were adopted, while higher temperatures, between 180 and 200 °C, were selected, because such polymeric solid substrate requires harsher reaction conditions than the glucose model compound to achieve satisfactory performances to BL. The results obtained for the butanolysis of PP are reported in Table 3.

The above data related to the experiments carried out in the Carius reactor show that at 190 °C an H_2SO_4 concentration of 1.2 wt % allowed a relevant BL production already after 1 h (35 mol %) and BL molar yield slightly improved up to 42 mol % after 3 h of reaction (runs PP1 and PP2, Table 3). On the other hand, the use of a lower acid concentration (0.6 wt %, runs PP3–PP6, Table 3) required longer reaction times to get appreciable BL formation, as better evidenced from the kinetics data reported in Fig. 5.

In fact, the best BL yield (34 mol %) was achieved only after 8 h but, noteworthy, a lower amount of DBE and solid residue than those achieved with the H_2SO_4 1.2 wt % was obtained after the same reaction time. This is a relevant aspect, because the presence of fewer by-products makes easier the separation and purification of BL. In addition, the etherification of *n*-BuOH to give DBE makes more complex its recycle, and the formation of both DBE and solid residue makes

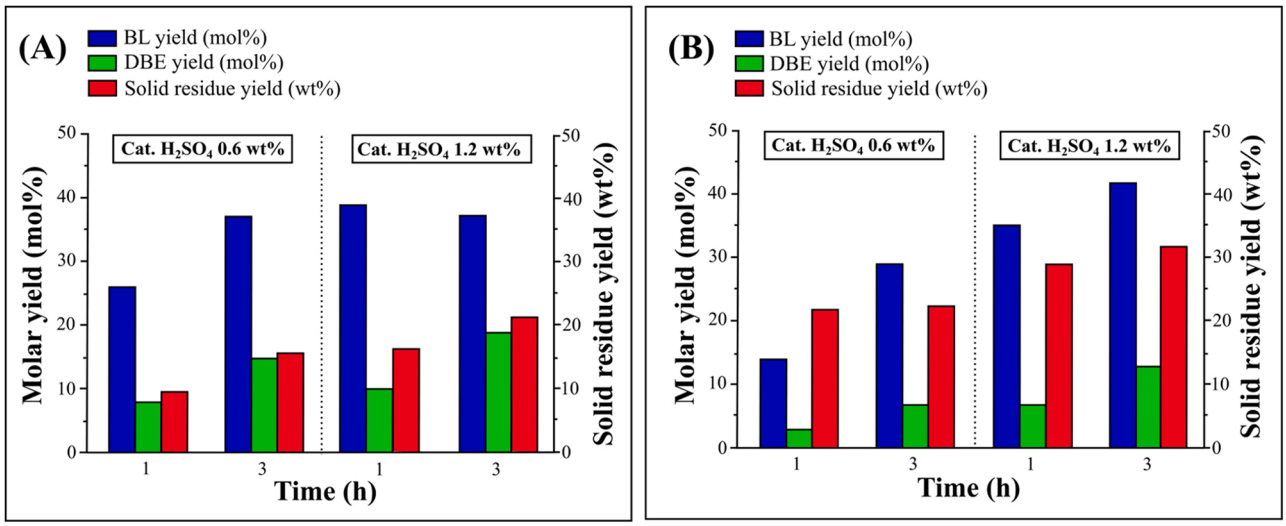

Fig. 6. Comparison between the butanolysis of: (A) MCC and (B) PP feedstocks. Reaction conditions: 190 °C, substrate loading of 14 wt %.

necessary their separation and disposal/valorisation, thus complicating the process. Moreover, the employment of a more diluted acid catalyst should be preferred to limit corrosion problems. Noteworthy, in all runs reported in Table 3 traces of furfural were also ascertained in the reaction mixtures: its formation is surely related to the dehydration of xylans present in low amount in the raw PP (12.1 wt %).

On the other hand, when the reaction was carried out in the autoclave at 190 °C with H_2SO_4 at 1.2 wt % (runs PP7–PP9, Table 3), longer reaction times than those previously reported for the reaction performed in Carius were necessary to achieve similar BL yields. For example, the BL molar yield of about 40 mol % was ascertained after 5 h in autoclave (run PP9, Table 3), whilst it was obtained after 3 h in Carius (run PP2, Table 3). However, in this case, longer reaction times did not promote the formation of by-products, as evidenced by the similar DBE and solid residue yields achieved in runs PP2 and PP9, highlighting that all the involved reactions were slowed down in autoclave. By halving the H_2SO_4 concentration for the runs performed in autoclave (runs PP10–PP12, Table 3), BL production was appreciable only after long reaction times, and the maximum BL molar yield of about 30 mol % was reached after 5 h of reaction, together with DBE molar yield and solid residue yield of 6 mol % and 21 wt %, respectively (run PP12, Table 3), analogously to the results obtained in Carius reactor after 3 h (run PP4, Table 3), thus evidencing also in this case that the reaction performed in autoclave is only slower than that carried out in Carius. Moreover, the influence of the reaction temperature was investigated in autoclave with the H_2SO_4 concentration of 0.6 wt %. When the reaction was carried out at the lower temperature of 180 °C for 5 h (run PP13, Table 3), the BL, DBE and solid residue yields were analogous to those already ascertained at 190 °C after the same reaction time (run PP12, Table 3), showing that the temperature decrease from 190° to 180°C did not affect the reaction selectivity. On the other hand, the temperature increase to 200 °C allowed the improvement of BL yield from 20 mol % (run PP11, Table 3) reached after 3 h at 190 °C, to 34 mol % after the same reaction time, but together with a higher by-products formation (DBE molar yield and solid residue yield of 7 mol % and 28 wt %, respectively) (run PP13, Table 3).

In conclusion, the switching from Carius to autoclave system did not significantly modify the product profile, thus the first one was further employed to proceed within this investigation, enabling us to reduce reaction time. In particular, to make further considerations on the reactivity of real cellulosic feedstocks towards butanolysis reaction, the most promising experiments already performed on the PP feedstock (runs PP1–PP4, Table 3), were replicated starting from the model clean microcrystalline cellulose (MCC), and the corresponding results are shown in Fig. 6.

Regarding the MCC butanolysis carried out with H_2SO_4 0.6 wt %, it was found that higher BL molar yields than those obtained from the corresponding PP butanolysis experiments were achieved after 1 and 3 h of reaction, respectively. On the other hand, when H_2SO_4 1.2 wt % was employed, more similar BL molar yields were obtained starting from MCC and PP. Moreover, regarding the production of by-products for both reaction times and H_2SO_4 concentrations, higher molar yields of DBE were observed when MCC was employed as feedstock. This result can be justified considering the presence of basic salts (ashes) in the starting PP, which are absent in MCC. They negatively affected the reaction, partially neutralising H_2SO_4 and consequently decreasing the

Table 4
Literature review on BL production starting from commercial cellulose.

Entry	Catalyst	Catalyst loading (wt %)	Cellulose loading (wt %)	T (°C)	Time (h)	BL Molar yield (mol %)	Ref.
1	H_2SO_4	2	11	210	0.17	40	[38]
2	H_2SO_4	20	1	130	20	60	[39]
3	H_2SO_4[a]	0.6	2	200	0.5	50	[43]
4	$Fe_2(SO_4)_3$	0.6	3	220	3	30	[34]
5	$Fe_2(SO_4)_3$+$Al_2(SO_4)_3$[a]	1+0.06	2	194	3	40	[42]
6	$Cs_2HPW_{12}O_{40}$[a]	1	2	200	1	12	[43]
7	SO_4^{2-}/ZrO_2[a]	1	2	200	1	13	[43]
8	SO_4^{2-}/SnO_2-ZrO_2+H_2SO_4	2+0.06	6	200	2	28	[36]
9	$[C_4H_8SO_3Hmim]HSO_4$[a]	1	9	180	0.75	31	[44]
10	H_2SO_4[a]	1.2	14	190	1	39	This work
11	H_2SO_4[b]	1.2	14	190	3	42	This work

[a] MCC adopted as substrate.
[b] PP adopted as substrate.

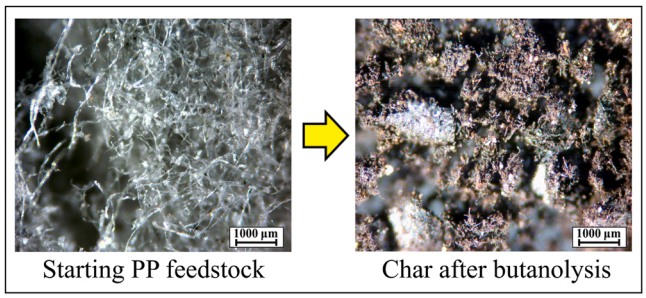

Fig. 7. Microscope images evidencing the texture change of the starting PP feedstock, as a consequence of the occurred butanolysis treatment.

acidity available for the reactions during the PP alcoholysis. On the other hand, the amounts of solid residue were always higher in the case of PP, due to the presence of lignin and xylans, this last producing, under the adopted temperature, furanic intermediates, which are quickly converted into soluble and insoluble condensation products [60]. On this basis, the tested model feedstock MCC resulted more prone towards BL production than PP, but the potential production of BL from waste biomasses, rather than from model compounds, is strongly preferable, due to the negative economic value of the first ones, which fully justifies their use for this reaction.

Finally, analogously to glucose, the best results obtained in the present work starting from MCC and PP (entries 10 and 11, Table 4) were compared with those already reported in the literature for the butanolysis of commercial cellulose to BL (Table 4).

Most of the available studies were performed starting from very low cellulose loadings (1–6 wt %) and only two works proposed higher values, equal to 11 and 9 wt % (entries 1 and 9, Table 4), which are lower than those investigated in the present study. Both homogeneous and *ad-hoc* synthesized heterogeneous acid catalysts have been employed in the literature, leading to BL yields in the range of 12–60 mol %, with the highest values reported for the butanolysis of cellulose catalyzed by 0.6–20 wt % H_2SO_4 (entries 1–3, Table 4). As previously reported for glucose, also in this case, the use of low concentrations of cellulose favors the BL production but produces too diluted BL streams, thus making not economically sustainable the scale-up. Under this perspective, the high-gravity approach adopted in this work acquires great relevance, in particular considering that the highest BL yields obtained starting from MCC and the real waste PP, equal to 39 and 42 mol % respectively (entries 10 and 11, Table 4), are comparable with those reported in the literature starting from lower starting substrate loadings (entries 1–9, Table 4).

3.3. Characterization of the char recovered after butanolysis of cellulosic feedstocks

To develop a fully integrated approach and promote the development of the alcoholysis process on a greater scale, it is necessary to consider the fate of the solid residue recovered after the reaction. In the case of the hydrothermal process, this carbonaceous residue is a char, which is immediately exploitable for the energy production or, more

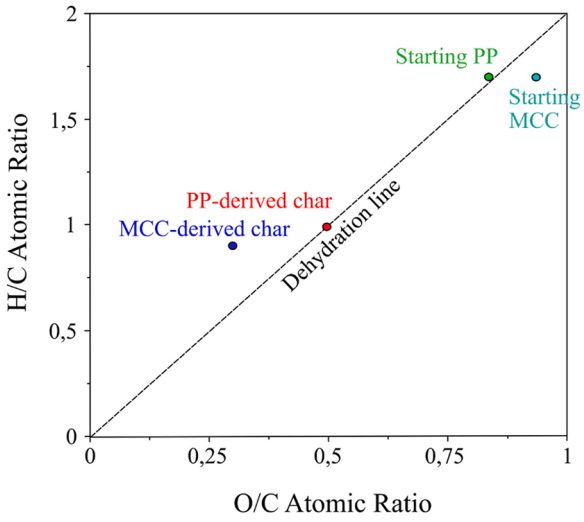

Fig. 8. Van Krevelen plot of the starting PP and MCC and the corresponding butanolysis-derived chars.

advantageously, for developing new applications in different fields of research, e.g. as adsorbent, carbon source for soil, filler in polymer, catalyst support and electrode for electrochemical energy storage [61]. Chemical composition of the hydrochar depends on the adopted starting feedstock, thus including only polyfuranic humins starting from simple sugar-based feedstocks [54,62,63], or (pseudo-lignin + humins), starting from more complex lignocellulosic feedstocks [64,65]. Moreover, also the solvent influences the char formation and the use of alcohols generally favors the stabilization of the involved reaction intermediates, thus strongly reducing the humin formation and leading to a less degraded and charred solid residue than that deriving from the thermal treatment performed in water medium [14,66]. The microscope image of the char recovered from the PP butanolysis confirms the textural changes of the raw PP feedstock as consequence of the butanolysis treatment (Fig. 7). In particular, the presence of small brown particles in the recovered char showed the occurred carbonization of the PP feedstock and the formation of humins, in agreement with the literature results [55]. On the other hand, the presence of small white regions in the char could indicate the presence of residual unconverted cellulose ribbons but also inorganic species. To better clarify this aspect, a more in-depth characterization of the bulk solid char has been proposed.

For this purpose, the solid residues produced from butanolysis of the PP and MCC feedstocks carried out under the same reaction conditions were characterized to get information about their chemical composition. In this regard, the char deriving from the best PP butanolysis test performed in autoclave (BL yield of 39 mol % and corresponding char yield of 31 wt %, according to run PP9, Table 3), was considered as the reference for the following investigation and its main physico-chemical properties were compared with those of the MCC-derived char synthesized under the same reaction conditions (BL yield of 37 mol % and corresponding char yield of 20 wt %).

First of all, the ultimate analysis of the starting PP and MCC

Table 5
Ultimate analysis of the starting PP and MCC feedstocks and their corresponding chars obtained by applying the same butanolysis treatments.

Sample	C (%)	H (%)	N (%)	S (%)	O (%)[a]	Ash (%)	O/C molar ratio	H/C molar ratio	HHV (MJ/kg)[b]
Starting PP	44.0	6.2	0.1	0.4	49.3	6.8	0.8	1.7	17.5
Starting MCC	42.0	5.9	0.0	0.0	52.1	0.0	0.9	1.7	16.2
PP-derived char	56.1	4.9	0.1	2.3	36.6	16.5	0.5	1.0	21.4
MCC-derived char	69.7	5.5	0.0	0.3	24.5	0.0	0.3	0.9	28.3

Note [a]: Oxygen content was calculated by difference: O (%) = 100 (%) – C (%) – H (%) – N (%).
Note [b]: HHV was calculated according to the correlation equation proposed by Channiwala et al. [53].

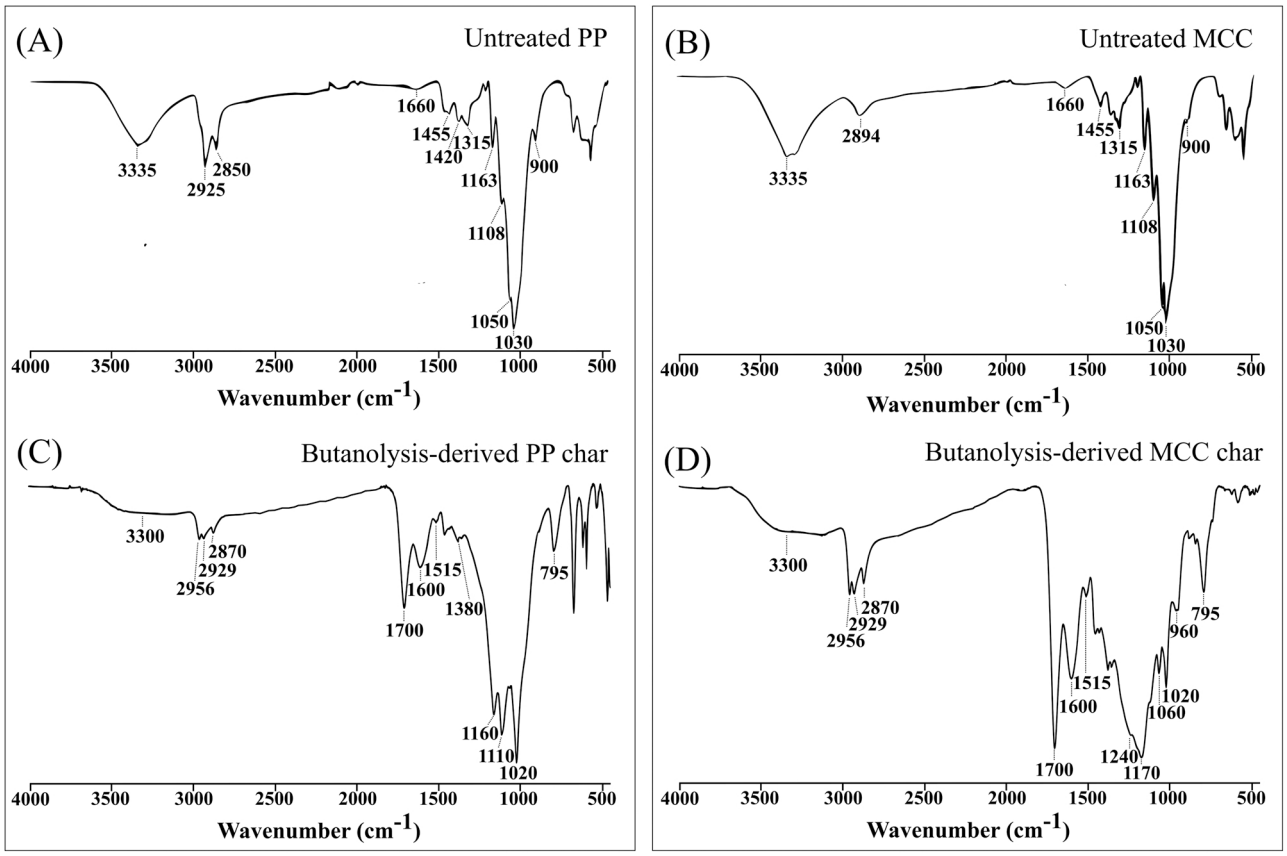

Fig. 9. FT-IR spectra of the starting raw PP (A) and MCC (B) feedstocks, and the corresponding butanolysis-derived chars (C and D, respectively).

feedstocks and their corresponding chars was carried out to evaluate the achieved degree of carbonization/deoxygenation of the two different feedstocks. The results are reported in Table 5, together with the corresponding calculated HHV data.

The above data confirm the bulk chemical similarity between the two starting feedstocks. Moreover, taking into account also the data related to the chars, the carbonization/deoxygenation of MCC was more advanced than that of PP, thus highlighting the higher reactivity of the former towards the dehydration path. Besides, similar O/C and H/C ratios have been obtained for both chars (see the Van Krevelen plot of Fig. 8), resulting in agreement with the results already reported in the literature for this kind of carbon-like materials, which are assimilable to traditional low-rank coals (e.g. lignite) [67–69].

The H/C and O/C atomic ratios of the starting feedstocks and the corresponding chars in the Van Krevelen diagram confirm that dehydration is the main allowed path, leading to the formation of carbonaceous humins [67,68]. Besides, the most significant deviation from the dehydration path occurred for the MCC feedstock, suggesting a more advanced degradation of this feedstock, whilst the degradation of the real PP biomass resulted less severe (higher O/C ratio).

FT-IR spectra of the raw PP and MCC feedstocks and the corresponding chars are reported in Fig. 9.

The comparison between the FT-IR spectra of the two starting feedstocks demonstrates their bulk chemical similarity. However, analogously to the butanolysis of glucose, also in this case, the alcoholysis reaction led to the formation of furanic humins. In the spectra of butanolysis-derived chars, the absorption bands at 1163 cm^{-1}, assigned to the C–O–C group stretching, and those between 1108 and 900 cm^{-1}, assigned to the ring valence vibrations of glucose, disappeared after the butanolysis treatment, thus indicating the disruption of the cellulose structure [55]. On the other hand, new absorption bands of furanic/aromatic source (humins) come out, which are the same previously observed for the butanolysis-derived glucose char (Fig. 3). In particular, the bands at 1600, 1515, 1379 and 795 cm^{-1}, whose assignments have been previously reported, are present in the spectra of the butanolysis-derived MCC and PP chars [54,55]. Moreover, also in these chars, the presence of oxygenated functionalities is shown by the bands at 1700 cm^{-1} and at 1240 and 1020 cm^{-1}, characteristic of the stretching of C═O of carbonyls and the stretching of C–O of ethers, respectively [54]. Noteworthy, the presence of the broad and weak absorption band of free OH groups (about 3300 cm^{-1}) is indicative of a limited reactivity of the functional groups of these chars, which have not undergone a bulk derivatization in the adopted *n*-BuOH solvent. In addition, in the case of the MCC-derived char, the absorption bands within 1700–1515 cm^{-1} are broader than those acquired for the PP-derived char. On the other hand, the IR spectrum of PP-derived char in the region between 1300 and 1000 cm^{-1}, which may indicate the presence of residual cellulose. All these observations highlight a more drastic structure change of the MCC feedstock, thus supporting the conclusion that PP char is less degraded than the MCC one, even if both chars have been synthesized under the same butanolysis conditions, in agreement with the results of the ultimate analysis.

Lastly, the XRD characterization of the PP-derived char has been carried out and the corresponding spectrum is reported in Fig. S2. This highlights the occurrence of an important deconstruction of bulk cellulose after the butanolysis treatment. In fact, the characteristic diffraction patterns of the crystalline cellulose (according to the XRD spectrum of the untreated PP) are no more present (Fig. S2A), thus confirming the amorphous structure of residual cellulose. On the other hand, due to the increased concentration of ashes in the PP-derived char, the diffraction patterns of inorganic compounds become more visible, thus further confirming the presence of $CaSO_4$ and, additionally, other signals due to minor compounds. Anyway, their intensities are comparable with the background noise (Fig. S2B and Table S2).

This preliminary characterization highlights that the produced chars could be ideally used for the energy recovery within the same BL process, thanks to their promising HHV values. However, the high sulphur concentration (2.3 wt %) of char obtained from the PP butanolysis could lead to SO_x emissions after its combustion, thus making this exploitation possibility not environmentally sustainable and practically uninteresting. Thus, more advantageously, they could be employed as starting materials for the synthesis of green adsorbents for new environmental applications. However, given the very low specific surface areas ($<10\ m^2/g$), these chars should require further physico-chemical activation post-treatments, in order to get efficient adsorbents, to use for the treatment of the wastewaters within the same papermill process which produces the PP waste. This further exploitation possibility is now under investigation.

4. Conclusions

In this paper, the one-pot catalytic butanolysis of a waste cellulose originating from a paper-mill process has been investigated and optimized. Such waste, which is still very rich in cellulose, is a suitable feedstock for the butyl levulinate production, working with *n*-butanol as the reagent/reaction medium, very dilute sulfuric acid as the homogeneous catalyst, and relatively mild reaction conditions. Yields up to about 40 mol % have been achieved as a consequence of this optimization study, working at the optimum feedstock loading of 14 wt %, which is higher than the majority of the loadings reported up to now, thus allowing the production of concentrated butyl levulinate streams. These results are promising, resulting in agreement with those obtained starting from model (but costly) microcrystalline cellulose, working at the same low catalyst loading (1.2 wt %). A preliminary characterization of the recovered chars has highlighted a slower degradation of the cellulose fraction in the case of the paper-mill waste, thanks to its fibrous texture. Moreover, this characterization has revealed that the obtained char is rich in oxygenated functionalities, making it an interesting green material to be used as the starting material for the production of new adsorbents. The combined production and exploitation of both butyl levulinate and char will make more sustainable and economically advantageous the one-pot catalytic butanolysis of this waste cellulosic biomass.

CRediT authorship contribution statement

Anna Maria Raspolli Galletti: Conceptualization, Methodology, Writing – original draft, Writing – review & editing. **Rosaria Lorè :** Methodology, Writing – review & editing. **Domenico Licursi:** Methodology, Writing – original draft, Writing – review & editing. **Nicola Di Fidio**: Methodology, Writing – review & editing. **Claudia Antonetti:** Conceptualization, Methodology, Writing – review & editing. **Sara Fulignati:** Conceptualization, Methodology, Writing – original draft, Writing – review & editing.

Declaration of Competing Interest

The authors declare that they have no known competing financial interests or personal relationships that could have appeared to influence the work reported in this paper.

Data availability

The data that has been used is confidential.

Acknowledgements

The authors are gratefully to the project PRIN 2017 (Progetti di Ricerca di Rilevante Interesse Nazionale) VISION “Development and promotion of the levulinic acid and carboxylate platforms by the formulation of novel and advanced PHA-based biomaterials and their exploitation for 3D printed green-electronics applications” (code FWC3WC_002) provided by Italian Ministero dell’Università e della Ricerca (MIUR).

This research was conducted within the activities of the RTD−A contract (no.1112/2021, Prot. no.0165823/2021) co-funded by the University of Pisa (Italy) in respect of the PON “Ricerca e Innovazione” 2014–2020 (PON R&I FSE-REACT EU), Azione IV.6 “Contratti di ricerca su tematiche Green”.

Appendix A. Supporting information

Supplementary data associated with this article can be found in the online version at doi:10.1016/j.cattod.2023.114054.

References

[1] K.A. Ahmad, M.H. Siddiqui, K.K. Pant, K. Nigam, N.P. Shetti, T.M. Aminabhavi, E. Ahmad, J. Chem. Eng. 447 (2022) 137550–137569.
[2] F. Oppong, C. Xu, X. Li, Z. Luo, Fuel Process. Technol. 229 (2022) 107185–107214.
[3] K. Alper, K. Tekin, S. Karagöz, A. Ragauskas, Fuels, Sustain. Energ. Fuels 4 (2020) 4390–4414.
[4] A. Démolis, N. Essayem, F. Rataboul, ACS Sustain. Chem. Eng. 2 (2014) 1338–1352.
[5] L. Yan, Q. Yao, Y. Fu, Green. Chem. 19 (2017) 5527–5547.
[6] G. Shrivastav, T.S. Khan, M. Agarwal, M.A. Haider, ACS Sustain. Chem. Eng. 5 (2017) 7118–7127.
[7] F.A. Freitas, D. Licursi, E.R. Lachter, A.M. Raspolli Galletti, C. Antonetti, T.C. Brito, R.S.V. Nascimento, Catal. Commun. 73 (2016) 84–87.
[8] A. Garcia-Ortiz, K.S. Arias, M.J. Climent, A. Corma, S. Iborra, ChemSusChem 13 (2020) 707–714.
[9] D. Zhao, Y. Wang, F. Delbecq, C. Len, Mol. Catal. 475 (2019) 110456–110461.
[10] L. Biancalana, S. Fulignati, C. Antonetti, S. Zacchini, G. Provinciali, G. Pampaloni, A.M. Raspolli Galletti, F. Marchetti, New J. Chem. 42 (2018) 17574–17586.
[11] A.S. Amarasekara, M.A. Animashaun, Catal. Lett. 146 (2016) 1819–1824.
[12] G.B. Kasar, N.S. Date, P. Bhosale, C.V. Rode, Energy Fuels 32 (2018) 6887–6900.
[13] D. Di Menno Di Bucchianico, Y. Wang, J.-C. Buvat, Y. Pan, V.C. Moreno, S. Leveneur, Green. Chem. 24 (2022) 614–646.
[14] X. Hu, C. Lievens, A. Larcher, C.-Z. Li, Bioresour. Technol. 102 (2011) 10104–10113.
[15] L. Shuai, J. Luterbacher, ChemSusChem 9 (2016) 133–155.
[16] A.M. Raspolli Galletti, C. Antonetti, S. Fulignati, D. Licursi, Catalysts 10 (2020) 1221–1281.
[17] Y. Ma, W. Tan, K. Wang, J. Wang, J. Jiang, J. Xu, ACS Sustain. Chem. Eng. 5 (2017) 5880–5886.
[18] R. Grisel, J. Van Der Waal, E. De Jong, W. Huijgen, Catal. Today 223 (2014) 3–10.
[19] Y. Ma, J. Wang, W. Tan, J. Jiang, J. Xu, K. Wang, Ind. Crops Prod. 135 (2019) 251–259.
[20] T. Zhao, Y. Zhang, G. Zhao, X. Chen, L. Han, W. Xiao, Fuel Process. Technol. 180 (2018) 14–22.
[21] G. Wu, C. Shen, S. Liu, Y. Huang, S. Zhang, H. Zhang, Green. Chem. 23 (2021) 9254–9282.
[22] J.F. Leal Silva, R. Grekin, A.P. Mariano, R. Maciel Filho, Energy Technol. 6 (2018) 613–639.
[23] L. di Bitonto, G. Antonopoulou, C. Braguglia, C. Campanale, A. Gallipoli, G. Lyberatos, I. Ntaikou, C. Pastore, Bioresour. Technol. 266 (2018) 297–305.
[24] T. Lei, Z. Wang, X. Chang, L. Lin, X. Yan, Y. Sun, X. Shi, X. He, J. Zhu, Energy 95 (2016) 29–40.
[25] V. Trombettoni, D. Lanari, P. Prinsen, R. Luque, A. Marrocchi, L. Vaccaro, Prog. Energy Combust. Sci. 65 (2018) 136–162.
[26] Z. Mohammadbagheri, A.N. Chermahini, Renew. Energy 147 (2020) 2229–2237.
[27] S. Jia, J. Ma, D. Wang, K. Wang, Q. Zheng, C. Song, X. Guo, Sustain. Energy Fuels 4 (2020) 2018–2025.
[28] G. Wang, Z. Zhang, L. Song, Green. Chem. 16 (2014) 1436–1443.
[29] F. Kremer, S. Pischinger, Butyl ethers and levulinates, in: M. Boot (Ed.), Biofuels from Lignocellulosic Biomass: Innovations beyond Bioethanol, Wiley-WCH, Weinheim, 2016, pp. 87–104.
[30] S. Frigo, G. Pasini, G. Caposciutti, M. Antonelli, A.M. Raspolli Galletti, S. Gori, R. Costi, L. Arnone, Fuel 297 (2021) 120742–120751.
[31] E. Christensen, A. Williams, S. Paul, S. Burton, R.L. McCormick, Energy Fuels 25 (2011) 5422–5428.
[32] K.C. Badgujar, V.C. Badgujar, B.M. Bhanage, Fuel Process. Technol. 197 (2020) 106213–106231.
[33] K.C. Badgujar, V.C. Badgujar, B.M. Bhanage, Catal. Today 408 (2023) 9–21.
[34] R. An, G. Xu, C. Chang, J. Bai, S. Fang, J. Energy Chem. 26 (2017) 556–563.
[35] D. Liu, L. Lin, S. Zeng, L. Peng, Chem. Ind. For. Prod. 33 (2013) 66–70.
[36] Y. Liu, L. Lin, D. Liu, J.P. Zhuang, C.S. Pang, Adv. Mater. Res. 955 (2014) 779–784.
[37] Z. Babaei, A.N. Chermahini, M. Dinari, Colloids Surf. A: Physicochem. Eng. Asp. 625 (2021) 126885–126894.
[38] K. Garves, J. Wood, Chem. Technol. 8 (1988) 121–134.

[39] Y. Hishikawa, M. Yamaguchi, S. Kubo, T. Yamada, J. Wood Sci. 59 (2013) 179–182.
[40] A. Démolis, M. Eternot, N. Essayem, F. Rataboul, ChemSusChem 10 (2017) 2612–2617.
[41] L. Zhou, D. Gao, J. Yang, X. Yang, Y. Su, T. Lu, Cellulose 27 (2020) 1451–1463.
[42] L. Deng, C. Chang, R. An, X. Qi, G. Xu, Cellulose 24 (2017) 5403–5415.
[43] A. Démolis, M. Eternot, N. Essayem, F. Rataboul, New J. Chem. 40 (2016) 3747–3754.
[44] H. Ma, J.X. Long, F.R. Wang, L.F. Wang, X.H. Li, Acta Phys. - Chim. Sin. 31 (2015) 973–979.
[45] T. Yamada, M. Yamaguchi, S. Kubo, Y. Hishikawa, Bioresources 10 (2015) 4961–4969.
[46] C. Antonetti, S. Gori, D. Licursi, G. Pasini, S. Frigo, M. López, J.C. Parajó, A. M. Raspolli Galletti, Catalysts 10 (2020) 509–530.
[47] M. Ouadi, A. Fivga, H. Jahangiri, M. Saghir, A. Hornung, Ind. Eng. Chem. Res. 58 (2019) 15914–15929.
[48] A. Sluiter, B. Hames, D. Hyman, C. Payne, R. Ruiz, C. Scarlata, J. Sluiter, D. Templeton, J. Wolfe, NREL/TP-510-42621, 9 (2008) 1–6.
[49] A. Sluiter, B. Hames, R. Ruiz, C. Scarlata, J. Sluiter, D. Templeton, D. Crocker, NREL/TP-510-42618, 1617 (2008) 1–16.
[50] A. Sluiter, B. Hames, R. Ruiz, C. Scarlata, J. Sluiter, D. Templeton, NREL/TP-510-42622, (2008) 1–6.
[51] A. Sluiter, R. Ruiz, C. Scarlata, J. Sluiter, D. Templeton, NREL/TP-510-42619, 1617 (2005) 1–9.
[52] S. Park, J.O. Baker, M.E. Himmel, P.A. Parilla, D.K. Johnson, Biotechnol. Biofuels 3 (2010) 1–10.
[53] S. Channiwala, P. Parikh, Fuel 81 (2002) 1051–1063.
[54] C. Rasrendra, M. Windt, Y. Wang, S. Adisasmito, I. Makertihartha, E. Van Eck, D. Meier, H. Heeres, J. Anal. Appl. Pyrolysis 104 (2013) 299–307.
[55] C. Chang, S. Wang, P. Guo, G. Xu, X. Zheng, C. Du, Y. Jiao, Chem. Eng. J. 453 (2023) 139873–139883.
[56] S. Saravanamurugan, A. Riisager, ChemCatChem 5 (2013) 1754–1757.
[57] L. Li, M. Wang, J. Ma, Z. Xu, Y. Zhang, S. Jia, Chem. Ind. For. Prod. 42 (2022) 135–146.
[58] Z. Babaei, R. Yazdanpanah Esmaeilabad, N. Orash, A. Najafi Chermahini, Biomass Convers. Biorefin. 1 (2020) 1–11.
[59] C. Xiros, M. Janssen, R. Byström, B.T. Børresen, D. Cannella, H. Jørgensen, R. Koppram, C. Larsson, L. Olsson, A.M. Tillman, Biofuels Bioprod. Biorefin. 11 (2017) 15–27.
[60] C. Antonetti, E. Bonari, D. Licursi, N. Nassi o Di Nasso, A.M. Raspolli Galletti, Molecules 20 (2015) 21232–21253.
[61] Z. Zhang, Z. Zhu, B. Shen, L. Liu, Energy 171 (2019) 581–598.
[62] G. Tsilomelekis, M.J. Orella, Z. Lin, Z. Cheng, W. Zheng, V. Nikolakis, D.G. Vlachos, Green. Chem. 18 (2016) 1983–1993.
[63] Z. Cheng, J.L. Everhart, G. Tsilomelekis, V. Nikolakis, B. Saha, D.G. Vlachos, Green. Chem. 20 (2018) 997–1006.
[64] D. Licursi, C. Antonetti, S. Fulignati, S. Vitolo, M. Puccini, E. Ribechini, L. Bernazzani, A.M. Raspolli Galletti, Bioresour. Technol. 244 (2017) 880–888.
[65] D. Licursi, C. Antonetti, J. Bernardini, P. Cinelli, M.B. Coltelli, A. Lazzeri, M. Martinelli, A.M. Raspolli Galletti, Ind. Crops Prod. 76 (2015) 1008–1024.
[66] N. Shi, Q. Liu, H. Cen, R. Ju, X. He, L. Ma, Biomass Convers. Biorefin. 10 (2020) 277–287.
[67] S. Wang, H. Lin, Y. Zhao, J. Chen, J. Zhou, J. Anal. Appl. Pyrolysis 118 (2016) 259–266.
[68] F. Björnerbäck, N. Hedin, ACS Sustain. Chem. Eng. 7 (2018) 1018–1027.
[69] O. Farobie, A. Amrullah, A. Bayu, N. Syaftika, L.A. Anis, E. Hartulistiyoso, RSC Adv. 12 (2022) 9567–9578.